Effects of Heat and Mass Transfer on the Flow of Nanofluids with Couple Stress Over Stretching Surfaces

Daniel Adams[1], William Walker[1], Olivia Davis[2], Amelia Wright[3], and Lucas Taylor*[3]

[1] Department of Geophysics, University of California, Berkeley, USA
[2] School of Biomedical Sciences, University of Sydney, Australia
[3] Department of Chemical Engineering, University of Manchester, UK

ABSTRACT

The present study to investigate the effects of heat and mass transfer flow in the presence of couple stress coefficient and Schmidt number using nanofluids over a stretching sheet. The governing partial differential equations are converted into ordinary differential equations with the help of similarity transformations and solved numerically by Shooting method using MAT lab subjected to the boundary conditions. The results are discussed through graphs and tables. It is observed that the present results are matched with the results by Gosh[16] and attained good agreement. We observed that both the nanofluid velocities increases due to increase in couple stress parameter. The concentration decreases for the increasing values of the stretching parameter ratio.

Key words: *Couple stress, Nanofluid, Stretching sheet, Heat transfer, Mass transfer, Radiation.*

Nomenclature:

a, b	stretching constants
B_0	magnetic flux
C	concentration of the fluid
D	mass diffusion coefficient
f	dimensionless stream function
f'	dimensionless velocity
K	coupled stress coefficient
k_f	thermal conductivity of the fluid
k_{nf}	effective thermal conductivity of the nanofluid
k_s	thermal conductivity of the solid
Pr	Prandlt number
q_r	radiative heat flux
R	radiation parameter
S	mass transfer parameter
Sc	Schmidt number
T	temperature of the fluid
u, v, w	fluid velocity components along x, y, z directions respectively

Subscripts:

nf	nanofluid
f	base fluid
s	solid
∞	quantities at free stream
w	quantities at wall

Greek symbols:

α_{nf}	thermal diffusivity of nanofluid

μ_{nf}	dynamic viscosity of nanofluid
ν_f	kinematic viscosity of the fluid
ν_{nf}	kinematic viscosity of the nanofluid
ν'_{nf}	couple stress viscosity of the fluid
ρ_{nf}	density of nanofluid
ϕ	volume fraction
σ	electrical conductivity
η	similarity variable
$(\rho C_p)_f$	heat capacitance of the fluid
$(\rho C_p)_{nf}$	heat capacity of the nanofluid
$(\rho C_p)_s$	heat capacitance of the solid
ρ_f	density of the fluid
ρ_s	density of the solid
τ_{zx}	wall shear stress along x-axis
τ_{zy}	wall shear stress along y-axis

I. INTRODUCTION

Now a days nanomaterials are being applied in many fields material sciences, electronics and medicine with potential applications. In recent years nanofluid has received great attention due to its unique properties. In general nanofluid is characterized as a base fluid with suspended solid nanoparticles of tiny size (1-100 nm) and nanofluid exhibits superior thermal conductivity and convective heat transfer coefficient when compared to the traditional fluids such as water, oil and ethylene glycol. Choi et al.[1]reported that the thermal conductivity of the conventional heat transfer fluid improved around two times when included with small nanoparticles even if the fraction is less than 1% of the volume. Due to enhanced heat transfer properties nanofluids find numerous applications in engineering processes especially in the cooling technologies. Das et al [2] analyzed the temperature dependence of the enhancement of thermal conductivity using nanofluids. Characteristics of boundary layer flow past a stretching sheet are studied by Khan et al.[3]using nanofluids.

Heat transfer technology stands at the cross roads of miniaturization on one hand and on the other hand astronomical increase in heat flux. Usually the enhancement techniques for heat transfer can hardly meet the challenge of ever increasing demand of heat removal in the processes involving electronic chips, laser applications etc. Heat transfer analysis is carried and analyzed by Nadeem et al.[4] over an exponentially stretching sheet for a water based nanofluid. Kakac et al.[5] investigated convective heat transfer enhancement using nanofluids. Strokes [6] and Devakar et al. [7] studied the effects of couple stress in fluids. Using couple stress squeeze flim the effects of surface roughness between a sphere and a flat plate are presented by Naduvinamani et al. [8]. Analytical solutions are derived by Devakar et al. [9] using slip boundary conditions for couple stress fluid flow. Najeeb et al. [10] and Srinivasacharya et al. [11] derived exact solutions for Magnetohydrodynamic flow of couple stress fluid. In a vertical porous layer Sreenadh et al. [12] examined the MHD free convection flow of couple stress. Heat and mass transfer flow at bodies of different shapes are analyzed by Vajravelu et al. [13]. An unsteady 3D flow of couple stress fluid is investigated by Hayat et al. [14] over a stretching sheet. In the presence of Newtonian heating Ramzan et al. [15] discussed 3D MHD flow of couple stress fluid. Sudipta Ghosh et al. [16] studied the couple stress effects on 3D flow of magnetic water based nanofluid past an extended surface.

Above literature motivated to study the couple stress effects of three dimensional heat and mass transfer flow in the presence of radiation using nanofluids over a stretching sheet. keeping this in mind a suitable similarity transformation are taken to convert the governing nonlinear partial differential equations into ordinary differential equations and applied shooting technique using MAT lab. The present results are matched with the results by Ghosh et al.[16] and obtained good agreement. The results are illustrated with the help of graphical representation and tabular representation.

II. MATHEMATICAL FORMULATION

We consider a steady three dimensional boundary layer flow of water based coupled stress incompressible nanofluid over a bidirectional linear stretching sheet in the presence of thermal radiation and concentration. Fig. 1 displays the geometrical representation of the present problem. We assumed that the stretching sheet has been stretched with the linear velocities u = ax, v = by, w = 0 along XYZ plane. Where u, v and w are the velocity components in the x, y, z directions respectively. T and C are the Temperature and concentration. ν is the viscosity. T_w, C_w are the temperature and concentration at the wall.

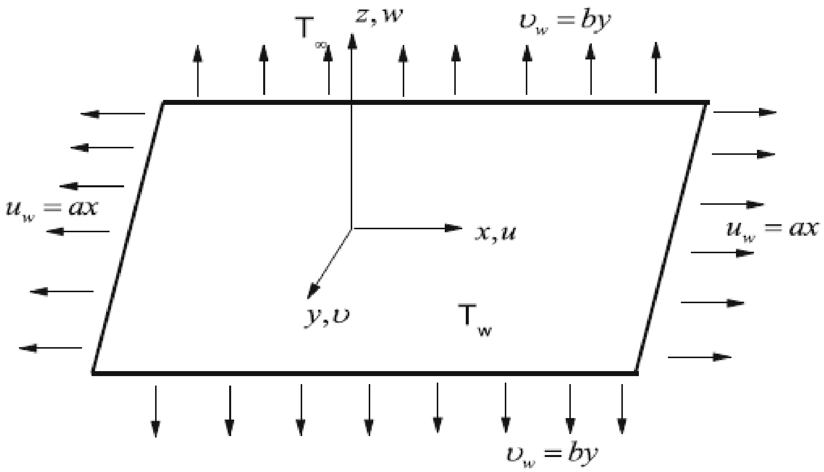

Fig .1 Geometrical representation of the problem

The governing equations under the above assumptions are given by

$$\frac{\partial u}{\partial x}+\frac{\partial v}{\partial y}+\frac{\partial w}{\partial z}=0 \tag{1}$$

$$u\frac{\partial u}{\partial x}+v\frac{\partial u}{\partial y}+w\frac{\partial u}{\partial z}=\nu_{nf}\frac{\partial^2 u}{\partial z^2}-\nu'_{nf}\frac{\partial^4 u}{\partial z^4} \tag{2}$$

$$u\frac{\partial v}{\partial x}+v\frac{\partial v}{\partial y}+w\frac{\partial v}{\partial z}=\nu_{nf}\frac{\partial^2 v}{\partial z^2}-\nu'_{nf}\frac{\partial^4 v}{\partial z^4} \tag{3}$$

$$u\frac{\partial T}{\partial x}+v\frac{\partial T}{\partial y}+w\frac{\partial T}{\partial z}=\frac{k_{nf}}{(\rho C_p)_{nf}}\frac{\partial^2 T}{\partial z^2}-\frac{1}{(\rho C_p)_{nf}}\frac{\partial q_r}{\partial z} \tag{4}$$

$$u\frac{\partial C}{\partial x}+v\frac{\partial C}{\partial y}+w\frac{\partial C}{\partial z}=D\frac{\partial^2 C}{\partial z^2} \tag{5}$$

subjected to the boundary conditions

$$u=u_w(x)=ax,\ v=v_w(y)=by,\ \frac{\partial^2 u}{\partial z^2}=0,\ \frac{\partial^2 v}{\partial z^2}=0,\ w=0,\ T=T_w,\ C=C_w \text{ at } z=0$$

$$u\to 0,\ \frac{\partial u}{\partial z}\to 0,\ v\to 0,\ \frac{\partial v}{\partial z}\to 0,\ T\to T_\infty,\ C\to C_\infty \text{ as } z\to\infty \tag{6}$$

where a > 0 and b > 0 for a stretching sheet.

The nanofluid properties are given by

$$\rho_{nf} = (1-\phi)\rho_f + \phi\rho_s, \quad (\rho C_p)_{nf} = (1-\phi)(\rho C_p)_f + \phi(\rho C_p)_s, \quad (\rho\beta)_{nf} = (1-\phi)(\rho\beta)_f + \phi(\rho\beta)_s,$$

$$\mu_{nf} = \frac{\mu_f}{(1-\phi)^{2.5}}, \quad K_{nf} = K_f \left\{ \frac{K_s + 2K_f - 2\phi(K_f - K_s)}{K_s + 2K_f + 2\phi(K_f - K_s)} \right\} \tag{7}$$

Table1: Thermophysical properties [5] of regular fluid and nanoparticles.

Physical properties	Regular fluid (water)	Cu
C_p (J/kg K)	4179	385
ρ (kg/m^3)	997.1	8933
κ (W/mK)	0.613	400
$\beta \times 10^{-5}$ (1/K)	21	1.67

The Rosseland approximation [4] radiative heat term is

$$q_r = \frac{-4\sigma^*}{3k^*}\frac{\partial T^4}{\partial z}, \; T^4 \cong 4T_\infty^3 T - 3T_\infty^4 \tag{8}$$

The similarity transformations are

$$u = axf'(\eta), \; v = ayg'(\eta), \; w = -\sqrt{a\nu_f}\left(f(\eta) + g(\eta)\right), \; \theta = \frac{T - T_\infty}{T_w - T_\infty}, C = \frac{C - C_\infty}{C_w - C_\infty}, \; \eta = \sqrt{\frac{a}{\nu_f}}z \tag{9}$$

The equations (2) to (5) are reduced to an ordinary differential equations using (6) to (9) as

$$Kf^{v} - \frac{1}{(1-\phi)^{2.5}\left(1-\phi+\phi\left(\frac{\rho_s}{\rho_f}\right)\right)} f''' - (f+g)f'' + (f')^2 = 0 \tag{10}$$

$$Kg^{v} - \frac{1}{(1-\phi)^{2.5}\left(1-\phi+\phi\left(\frac{\rho_s}{\rho_f}\right)\right)} g''' - (f+g)g'' + (g')^2 = 0 \tag{11}$$

$$(A+R)\theta'' + \Pr\left(1-\phi+\phi\left(\frac{(\rho C_p)_s}{(\rho C_p)_f}\right)\right)(f+g)\theta' = 0 \tag{12}$$

$$C'' + Sc(f+g)C' = 0 \tag{13}$$

where $K = \frac{a\nu'_{nf}}{\nu_f^2}$, $\Pr = \frac{(\mu C_p)_f}{K_f}$, $R = \frac{16\sigma^* T_\infty^3}{3k^* k_f}$, $Sc = \frac{\nu_f}{D}$, $A = \frac{K_{nf}}{K_f}$

and the corresponding boundary conditions are

$$f(\eta)=0,\; f'(\eta)=1,\; f'''(\eta)=0,\; g(\eta)=0, g'(\eta)=\lambda,\; g'''(\eta)=0, \theta(\eta)=1,\; C(\eta)=1 \text{ at } \eta=0$$
$$f'(\eta)\to 0,\; f''(\eta)\to 0,\; g'(\eta)\to 0,\; g''(\eta)\to 0,\; \theta(\eta)\to 0,\; C(\eta)\to 0 \text{ as } \eta\to\infty \tag{14}$$

where $\lambda = \frac{b}{a}$.

The physical quantities of interest [20]are as follows.

Skin friction coefficient along x-axis, $Cf_x = \frac{\tau_{zx}}{\rho_f u_w^2} \Rightarrow Cf_x \mathrm{Re}_x^{1/2} = \frac{1}{(1-\phi)^{2.5}} f''(0) - Kf^{iv}(0)$ (15)

Skin friction coefficient along y-axis, $Cf_y = \dfrac{\tau_{zy}}{\rho_f v_w^2}$

$$\Rightarrow Cf_y \operatorname{Re}_y^{1/2} = \frac{1}{\lambda^{3/2}} \frac{1}{(1-\phi)^{2.5}} g''(0) - \frac{1}{\lambda^{3/2}} K g^{iv}(0) \tag{16}$$

Nusselt number, $Nu = \dfrac{x q_w}{k_f (T_w - T_\infty)} \Rightarrow Nu \operatorname{Re}_x^{-1/2} = -A(1+R)\theta'(0)$ (17)

Sherwood number, $Sh = \dfrac{x q_m}{D(C_w - C_\infty)} \Rightarrow Sh \operatorname{Re}_x^{-1/2} = -C'(0)$ (18)

Where $\tau_{zx} = \mu_{nf} \dfrac{\partial u}{\partial z} - n \dfrac{\partial^3 u}{\partial z^3}$, $\tau_{zy} = \mu_{nf} \dfrac{\partial v}{\partial z} - n \dfrac{\partial^3 v}{\partial z^3}$, $q_w = -k_{nf}(1+R)\dfrac{\partial T}{\partial z}$, $q_m = -D \dfrac{\partial C}{\partial z}$.

III. RESULTS AND DISCUSSION

The ordinary differential equations from (10) to (13) subjected to the boundary conditions (14) are solved numerically by Shooting method using MAT lab. In the present work we have studied the heat and mass transfer effects of an incompressible nanofluid in the presence of coupled stress coefficient, radiation parameter and Schmidt number. To study the effects of various parameters we have used the copper based nanofluid to enhance the thermal properties and the volume fraction at 0 and 0.01.

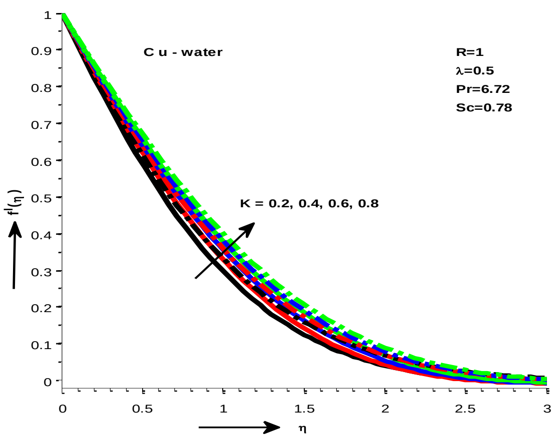

Fig.2(a). Effects of Coupled stress parameter on Primary velocity

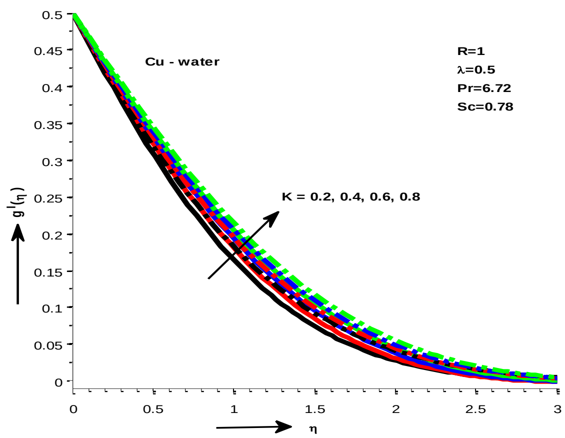

Fig.2(b) Effects of Coupled stress parameter on secondary velocity

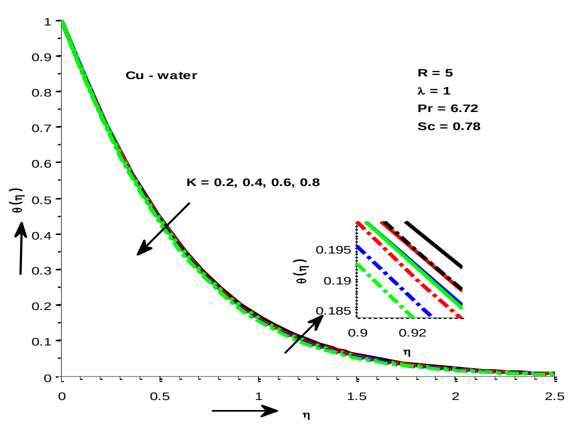

Fig.2(c) Effects of Coupled stress parameter on temperature.

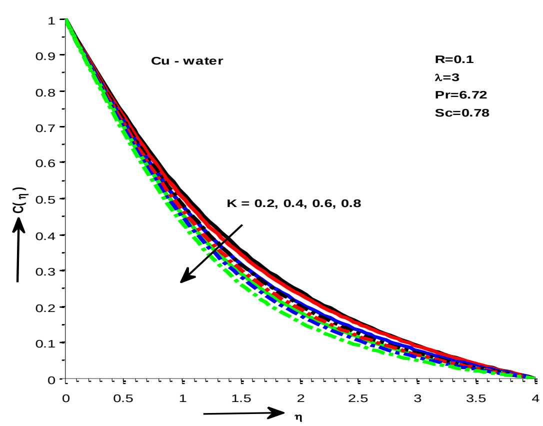

Fig.2(d) Effects of Coupled stress parameter on *concentration.*

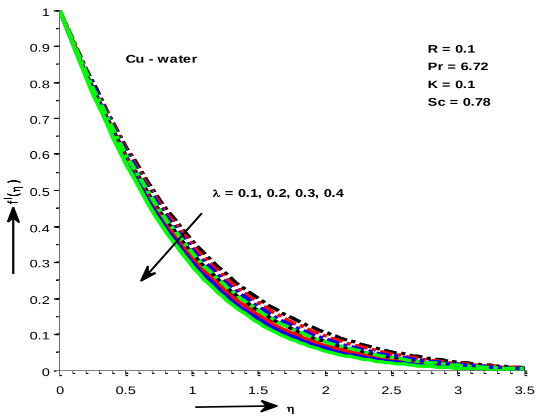

Fig.3(a) Effects of Stretching parameter ratio on primary velocity.

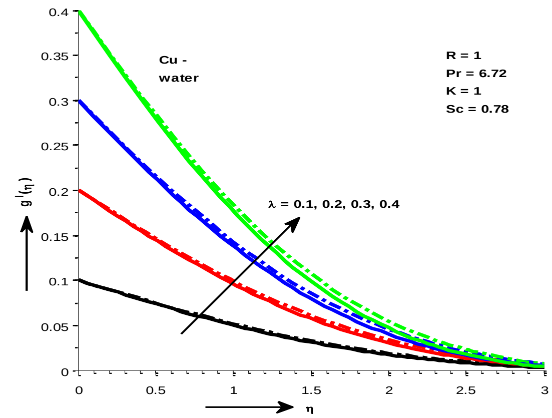

Fig.3(b) Effects of Stretching parameter ratio on secondary velocity.

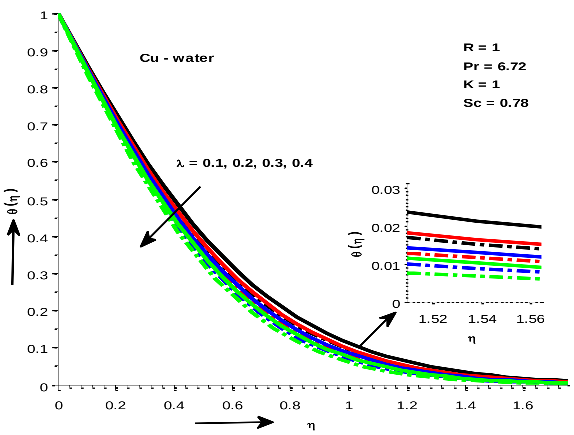

Fig.3(c) Effects of Stretching parameter ratio on temperature.

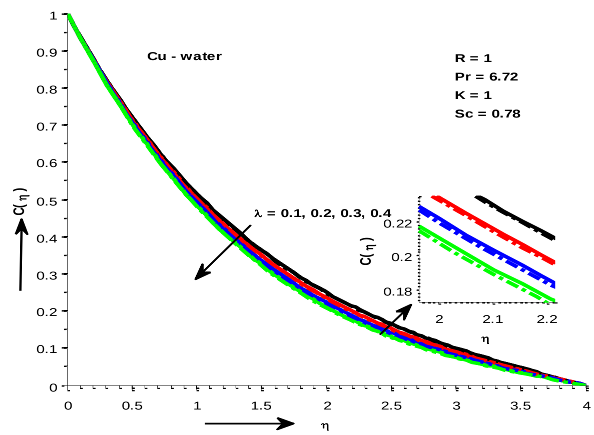

Fig.3(d) Effects of Stretching parameter ratio on concentration.

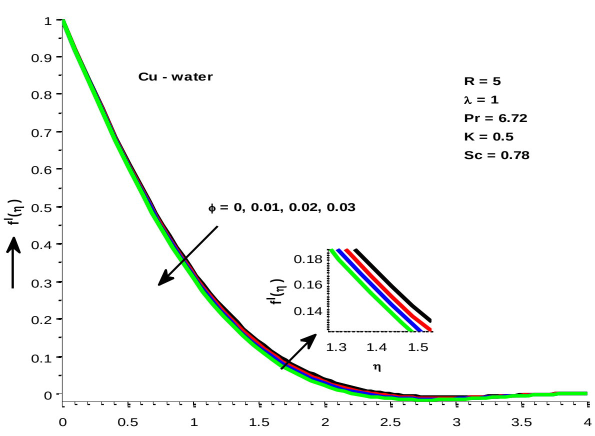

Fig.4(a) Effects of volume fraction parameter on primary velocity.

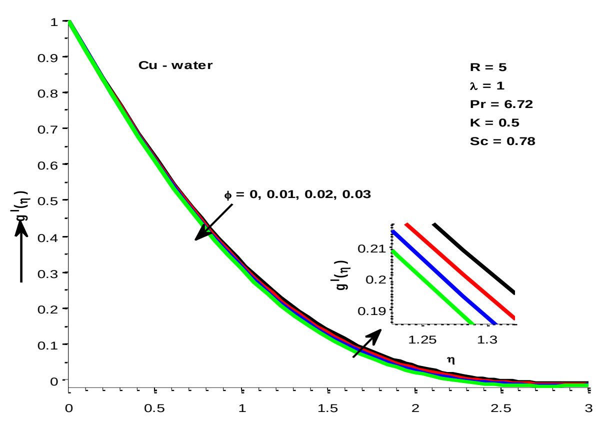

Fig.4(b) Effects of volume fraction parameter on secondary velocity.

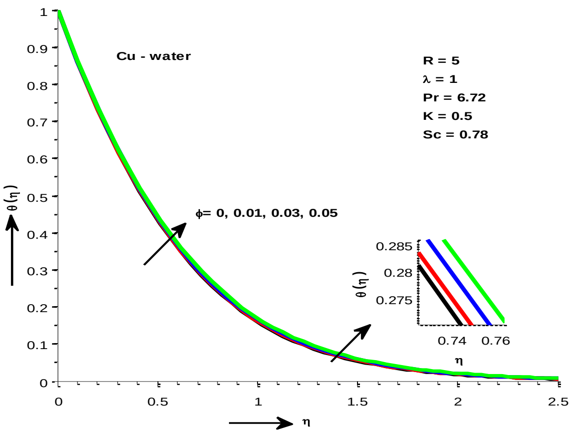

Fig.4(c) Effects of volume fraction parameter on temperature.

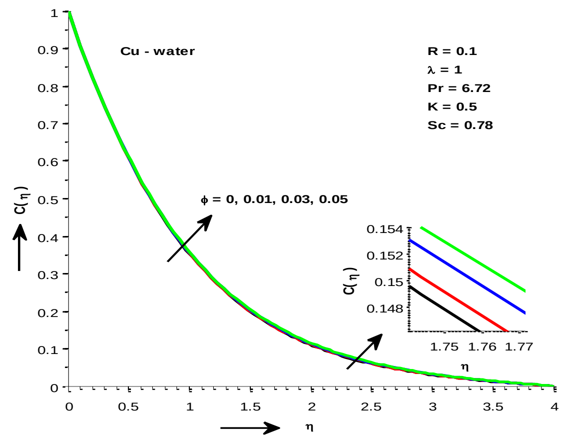

Fig.4(d) Effects of volume fraction parameter on concentration.

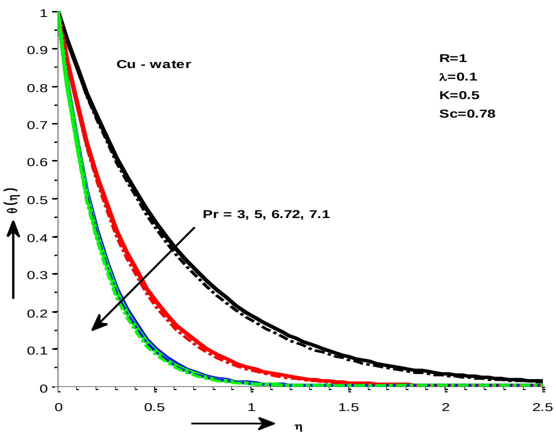

Fig.5 Effects of Prandtl number on temperature.

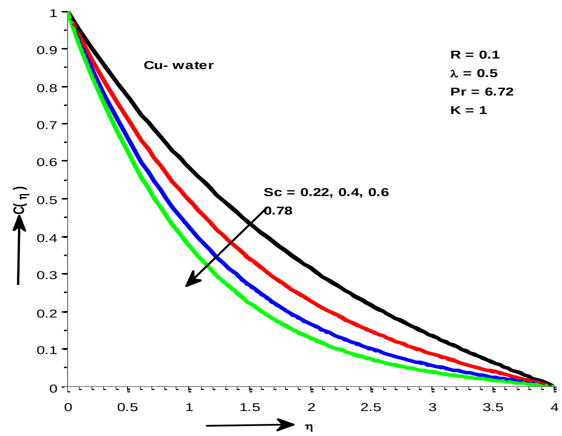

Fig.6 Effects of Schmidt number on Concentration

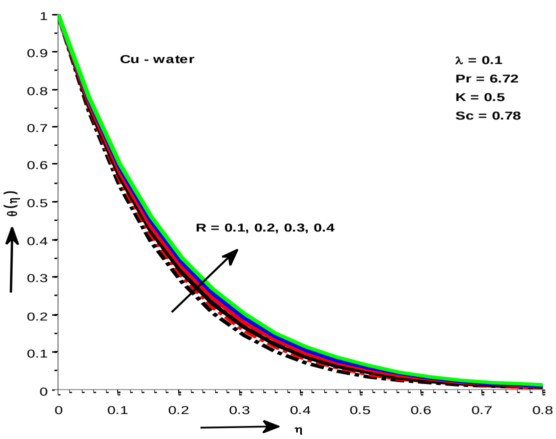

Fig.7 Effects of radiation parameter on temperature.

Fig.2(a) to 2(d) depicts the velocity profiles, temperature profiles and concentration profiles respectively for various values of Couple Stress parameter using copper water nanofluid. It is clear that both the velocities increases initially for the increasing values of coupled stress parameter but later both the velocities decreases for the increasing values of couple stress parameter. Hence the nanofluid velocity displays dual behavior with the influence of couple stress parameter. Viscosity effect is more near the surface and it is negligible far away from the surface. Therefore the rise in couple stress parameter results in the decrease in both the velocities. So the fluid becomes more viscous with the rise in couple stress coefficient, since couple stress parameter is associated to the couple stress viscosity. Hence retardation in fluid motion is noticed. The nanofluid temperature and concentration also decreases with the improved values of couple stress parameter. Hence the boundary layer thickness becomes thicker. Table 2 shows the effects of Couple Stress coefficient on Skin friction coefficient about both the axes, Nusselt number and Sherwood number. It is clear that Skin friction coefficient about x-axis decreases and increases about y-axis and Nusselt number and Sherwood number increases with an increase in Couple Stress parameter.

Effect of Stretching ratio parameter on both the velocities, temperature and concentration are represented in Figs.3(a) to 3(d) respectively. It shows that the primary velocity decreases with the increase in stretching ratio parameter but it exhibits reverse effect on secondary velocity. The same result was observed by Ghosh et al.[20] . Temperature and concentration decreases with an increase in stretching ratio parameter. Hence an increase in stretching ratio parameter helps in the enhancement of heat transfer rate and mass transfer rate. Hence the thermal boundary layer becomes thinner and attained good agreement. Physical quantities of interest are represented in the table 2 for the increasing values of stretching ratio parameter. Table 3 illustrates that there is a good agreement.

Figures from 4(a) to 4(d) depicts the effects of volume fraction on both velocities, temperature and concentration. It is evident that both the velocities decrease with the increase in volume fraction and temperature and concentration increases with the increase in volume fraction. The effects of Prandtl number on temperature are shown in Fig.5 and it is clear that the temperature decreases for the increasing values of the Prandtl number. From Fig.6 we noticed that the concentration decreases for the increasing values of Schmidt number. The effects of radiation parameter on temperature are displayed in Fig.7 and we observed that the temperature increases for the increasing values of the radiation parameter. Table 2 illustrates effects of radiation parameter on Nusselt number. We observed that Nusselt number increases with the increase in radiation parameter. The results on the effect of radiation parameter coincides with the results presented by Ghosh[20] and obtained good conformity.

Table 2: The effects of Skin friction coefficient about x-axis and y-axis, Nusselt number and Sherwood number for different values of Couple stress coefficient, Stretching ratio parameter, Radiation parameter, Heat source parameter, Schmidt parameter, chemical reaction parameter and Volume fraction are as follows.

K	λ	Pr	R	Sc	ϕ	$Cf_x \mathrm{Re}_x^{1/2}$	$Cf_y \mathrm{Re}_y^{1/2}$	$Nu \mathrm{Re}_x^{1/2}$	$Sh \mathrm{Re}_x^{1/2}$
0.2	0.1	6.72	1	0.78	0.05	-1.278840	-2.350342	9.591653	0.892734
0.4						-1.304286	-2.205666	9.595621	0.893216
0.6						-1.325628	-2.105436	9.598207	0.893601
0.8						-1.344548	-2.029774	9.600176	0.893919
0.5						-1.315341	-2.151673	9.597034	0.893418
	0.2					-1.343430	-1.648173	9.639176	0.901606
	0.3					-1.370973	-1.461608	9.681022	0.909330
	0.4					-1.398058	-1.379840	9.722858	0.916652
	0.1	3				-1.315341	-2.151673	6.398184	0.893418
		5				-1.315341	-2.151673	8.272305	0.893418
		6.72				-1.315341	-2.151673	9.597034	0.893418
		7.1				-1.315341	-2.151673	9.865858	0.893418
		6.72	0.1			-1.315341	-2.151673	6.921735	0.893418
			0.2			-1.315341	-2.151673	7.266475	0.893418
			0.3			-1.315341	-2.151673	7.596098	0.893418
			0.4			-1.315341	-2.151673	7.912379	0.893418
			1	0.22		-1.315341	-2.151673	9.597034	0.495730
				0.4		-1.315341	-2.151673	9.597034	0.646674
				0.6		-1.315341	-2.151673	9.597034	0.785439
				0.78		-1.315341	-2.151673	9.597034	0.893418
					0	-1.163414	-1.801278	8.620293	0.893830
					0.01	-1.194691	-1.870742	8.812588	0.893725
					0.02	-1.225327	-1.940225	9.006377	0.893633
					0.03	-1.255534	-2.010045	9.201679	0.893552

Table 3: Comparison of Skin friction coefficient about x-axis and y-axis , Nusselt number for various parameters such as Couple stress coefficient and Volume fraction in the absence of Schmidt parameter.

K	ϕ	$Cf_x \mathrm{Re}_x^{1/2}$		$Cf_y \mathrm{Re}_y^{1/2}$		$Nu \mathrm{Re}_x^{1/2}$	
		Present results	Results by Ghosh [20]	Present results	Results by Ghosh [20]	Present results	Results by Ghosh [20]
0.2	0.05	-1.278840	-1.278840	-2.350342	-2.350367	2.929582	2.929582
0.4		-1.304286	-1.304286	-2.205666	-2.205687	2.969899	2.969900
0.6		-1.325628	-1.325629	-2.105436	-2.105436	2.997733	2.997740
0.8		-1.344548	-1.344549	-2.029774	-2.029773	3.018703	3.018714
0.5	0	-1.163414	-1.163414	-1.801278	-1.801315	2.728596	2.728604
	0.01	-1.194691	-1.194691	-1.870742	-1.870742	2.779086	2.779093
	0.02	-1.225327	-1.225328	-1.940225	-1.940224	2.829980	2.829987
	0.03	-1.255534	-1.255535	-2.010045	-2.010045	2.881256	2.881263

IV. CONCLUSION

In the present study we have studied the heat and mass transfer effects of an incompressible nanofluid in the presence of coupled stress coefficient, radiation parameter and Schmidt number using Cu-water nanofluid by the solving obtained ordinary differential equations by Shooting method using MAT lab. The effects of various parameters for cu-water nanofluid with the volume fraction 0 and 0.01 are studied through tabular and graphical representation. The following are the conclusions from the present study.

1. For the increasing values of coupled stress parameter both the velocities increases initially and decreases finally but temperature and concentration decreases with the rise in coupled stress parameter. Hence the boundary layer thickness increases.
2. It is evident that the secondary velocity is increasing for the increasing values of coupled stress coefficient and stretching parameter ratio.
3. The nanofluid temperature increases for the increasing values of radiation parameter and stretching parameter ratio where as it decreases for the increasing values of Prandtl number.
4. Concentration and temperature increases with the increase in nanoparticle volume fraction.

REFERENCES

1. *Choi S.U.S, Zhang Z. G, Yu W, Lockwood F. E, Grulke E. A, "Anomalous Thermal Conductivity Enhancement in Nanotube Suspensions," Applied Physics Letters, 79, (2001). 2252.* http://dx.doi.org/10.1063/1.1408272
2. *Das S.K, Putra N, THiesen P, Roetzel W, "Temperature dependence of Thermal Conductivity Enhancement for Nanofluids," Journal of Heat and Mass Transfer, 125,(2003), 567-574.* http://dx.doi.org/10.1115/1.1571080
3. *Khan W. A, Pop I, "Boundary Layer Flow of a Nanofluid Past a Stretching sheet," International Journal of Heat and Mass Transfer, 53(11-12), 2010, 477-2483.* http://dx.doi.org/10.1016/j.ijheatmasstransfer.2010.01.032
4. *Nadeem S, Ul Haq R, Khan Z.H, "Heat Transfer Analysis of Water-based Nanofluid over an Exponentially Stretching Sheet," Alexandria Engineering Journal, 53(1), 2014, 219-224.* http://dx.doi.org/10.1016/j.aej.2013.11.003
5. *Kakac S, Pramuanjaroenkii A, "Review of Convective Heat Transfer Enhancement With Nanofluids", Int.J.HeatMass Transf, 52, 2009, 3187-3196.*
6. *Strokes V. K, "Couple Stresses In Fluids", Phys.Fluids, 9, 1966, 1709-1715.*
7. *Devakar M, Iyengar T. K. V, "Run up flow of a Couple Stress fluid between parallel plates", Non-Linear Anal.:Model. Control, 15, 2010, 29-37.*
8. *Naduvinamani N. B, Hiremath P. S, Gurubasavaraj G, :Effects of Surface Roughness on the Couple Stress Squeeze Flim Between a Sphere and a flat Plate", Tribol. Int. 38, 2005, 451- 458.*
9. *Devakar M, sreenivasulu D, Shankar B, "Analytical Solutions of Couple Stress Fluid Flows With Slip Boundary Conditions", Alexandria Engineering Journal, 53, 2014, 723 - 730.*
10. *Najeeb Alam Khan, Hassam Khan, Syed Anwar ali, "Exact Solutions for MHD Flow of Couple Stress Fluid With Heat Transfer", Journal of the Egyptian Mathematical Society, 24, 2016, 125-129.*

11. *Srinivasacharya D, Kaladhar K, "Analytical Solution of MHD Free Convective Flow of Couple Stress Fluid in an annulus With Hall and lon - slip effects ", Nonlinear Anal.:Model.Control, 16(4), 2011, 477-487.*
12. *Sreenadh S, Kishore S. N, Srinivas A. N. S, Reddy R. H ,"MHD Free Convection Flow of Couple Stress in a Vertical Porous Layer," Adv. Appl. Sci. Res.2(6), 2011, 215-222.*
13. *Vajravelu K, Mukhopadhayay S , "Fluid Flow, Heat and Mass Transfer at Bodies of Different Shapes:Numerical Solutions," Elsevier, Oxford, ISBN 978-0-12-803733-1, 2015.*
14. *Hayat T, Awais M, Safdar A, Hendi A. A, "Unsteady Three Dimensional Flow of Couple Stress Fluid Over a Stretching Surface With Chemical Reaction," Nonlinear Analysis: Modelling and Control ,17(1), 47-59, 2012.*
15. *Ramzan M, Farooq M, Alsaedi A, Hayat T', "MHD Three Dimensional Flow of Couple Stress Fluid With Newtonian Heating," Eur. Phys. J. Plus, 128, 2013, 49-63.*
16. *Sudipta Ghosh, Swati Mukopadhyay, Taswar Hayat, "Couple stress effects on three dimensional flow of magnetic-water based nanofluid over an extended surface in presence of non-linear thermal radiation," Int J. Appl. Comput. Math , 2018, 4:11.*